Available online at www.sciencedirect.com
ScienceDirect
Ceramics International 36 (2010) 1373–1381
CERAMICS INTERNATIONAL
www.elsevier.com/locate/ceramint

Cavitation and rolling wear in silicon nitride

B. Karunamurthy [a], M. Hadfield [a,*], C. Vieillard [b], G.E. Morales-Espejel [b], Z. Khan [a]

[a] *Sustainable Design Research Centre, School of Design, Engineering and Computing, Bournemouth University, Poole House, Bournemouth BH12 5BB, UK*
[b] *SKF Engineering and Research Centre B.V., Nieuwegein, The Netherlands*

Received 26 October 2009; received in revised form 19 November 2009; accepted 24 January 2010
Available online 1 March 2010

Abstract

Rolling contact and cavitation testing were integrated in a testing methodology to study their combined effect on silicon nitride rolling elements. This testing methodology is well suited to perform controlled cavitation and rolling contact experiments. Acoustic cavitation method and a rotary tribometer were utilized to achieve this objective. Silicon nitride degradation initiated with the formation of blisters in rolling contact. This blisters underwent cracking in the subsequent testing, thereby allowing the lubricant to squeeze in due to rolling contact. Erosion pits formed and their density increased along with their growth by detaching grains and bridging into adjacent pits. As the erosion severity in the rolling contact increased the material eventually failed in a short period of time with respect to the testing conditions. The effect of cavitation and rolling contact parameters on material damage is detailed in this paper thereby allowing an evaluation of material systems for cavitation-rolling contact fatigue (RCF) conditions.

Keywords: Rolling contact; Cavitation erosion; Silicon nitride; Wear

1. Introduction

One of the remarkable advancements in bearing technology is the development of hybrid bearings, which consists of silicon nitride rolling elements and steel races. This bearing offers several advantages over all-steel bearing and has shown extended rolling contact life [1–3]. Hybrid bearings have shown promising results when operated in cryogenic fluids such as liquid hydrogen, liquid oxygen and liquid nitrogen, as conditions required for high-speed turbo pumps in rocket engine for space applications [4–6]. Structural design and flow conditions in these conditions promote huge pressure variations, which result in cavitation, causing material damage. Material wear due to cavitation along with rolling contact fatigue is a complex phenomenon and a detailed experimental investigation on this effect was not reported. Correlation between rolling contact fatigue resistance and cavitation erosion was first reported in 1970 [7], arguing whether cavitation erosion is a contributing factor in the initiation of surface fatigue under lubricated high-stress rolling contact. This was followed by a report on the formation of spherical particles in rolling contact fatigue, could have been a result of cavitation [8]. Several publications are available on the wear of mechanical systems and also on the rolling contact fatigue experiments with refrigerant-oil mixture lubrication [9–12]. The liquid/gas phase transition has a significant influence on the wear mechanisms and need to be investigated [13]. Cavitation certainly occurs in the trailing edge of the rolling contact, but how cavitation affects the material damage in rolling contact is unclear. Therefore, a controlled level of liquid/gas phase in the lubricant during rolling contact experiments must be achieved to understand the influence of cavitation in rolling contact. The wear mechanism of rolling elements due to this integrated testing methodology is detailed in this paper. An integrated experimental approach allows concurrent conditions of concentrated rolling contact with thin-film lubrication studies with cavitation. The integrated test method reported in this paper also allows performing controlled rolling contact experiments with a wide range of loads and speeds, and varying intensity of cavitation.

2. Experimental methodology

Several factors influence the rolling contact life of bearing elements such as loading conditions, lubrication, surface

* Corresponding author. Tel.: +44 1202 965983; fax: +44 1202 965314.
E-mail address: mhadfield@bournemouth.ac.uk (M. Hadfield).

0272-8842/$36.00
doi:10.1016/j.ceramint.2010.02.011

contacts, materials and surface defects. Different testing methods are available for rolling contact fatigue experiments [14,15]. A Plint high-speed TE92 with four-ball rolling capability and microprocessor controlled rotary tribometer was used for this work and has been very successful for performing rolling contact fatigue experiments [16]. This rotary tribometer can simulate the running conditions of an angular contact ball bearing configuration under different conditions of contact stress and lubrication. The main components of this tribometer are the test chamber, the loading piston, the drive spindle and related bearings which are lubricated with grease for life. Rolling contact fatigue tests in a wide range of speeds and loads is possible with the control and instrumentation. The test chamber is a steel cup of 50 mm outer diameter supported by a steel cylinder to allow fastening of the steel cup to the machine. Three balls representing a planetary motion were placed inside the cup which was then filled with the test lubricant. Load is applied through a rotating shaft from the top which at the end has a collet to fix a fourth test rolling element. All test materials used are commercially available and are ground and polished to a diameter of 12.7 mm. The silicon nitride rolling elements has an elastic modulus and Poisson ratio of 310 GPa and 0.28 respectively with an average surface roughness (R_a) of 0.01 μm. The steel balls used were carbon chromium steel with the same diameter with an average surface roughness (R_a) of 0.02 μm. The hardness of silicon nitride and steel balls was 16.05 and 8.23 GPa, respectively.

In order to incorporate cavitation in this tribometer, different cavitation generating methods were investigated. Hydrodynamic methods, which are characterised by high-speed liquids passing through geometry restrictions, cannot be adapted mainly due to their test rig size. Other option such as rupturing the test liquid using high intensity light such as Light Amplified by Stimulated Emission of Radiation (LASER) is not cost effective. Vibratory cavitation method is well suited for this application and hence this method was customized by altering the cup design which fit to this test rig. A 5 mm diameter piezoelectric transducer was custom designed, and manufactured by a commercial supplier. This transducer vibrates to a maximum of 60 μm peak to peak with a maximum power of 600 W and operates at a resonance frequency of 20 kHz. An ultrasonic generator drives this piezoelectric transducer at the desired vibration and power, which can be continuously monitored. The only option to apply cavitation to the test chamber is by inserting the transducer through the sideways of the steel cup. This allows the transducer to be positioned close to the rolling elements enough to cause cavitation. The accurate position was determined by considering the tolerance between the face of the transducer and the test sample and also the dynamics of the lower balls. Any mild contact with the test sample or the lower balls will damage both the transducer and test materials due to abrasion. This test setup is shown in Fig. 1.

A port was created on the steel cup to ensure placing the transducer at the preferred location. A new AISI 316 stainless steel cup of the same design was manufactured and a port was created by using a high carbide drill bit. The reason to choose stainless steel as the material for the test chamber was mainly because of its superior resistance to cavitation [15]. This port was designed to a diameter of 5.5 mm in such a way that it accommodates the transducer horn which is of 5 mm in diameter with good tolerance. Mechanical sealants are not suitable to seal off the port from any lubrication leakage since the transducer should be free from any firm contact. Therefore, a high temperature adhesive sealant was selected which was first used to fill the port and allowed curing for 24 h. The centre of the port with the filled-in sealant was then carefully marked and a hole of 4 mm diameter was created. This allowed inserting the transducer with less pressure. This sealant is very important as it allow fixing the transducer to the test chamber, seals off the port for any lubrication leakage and allows the transducer to vibrate effectively to achieve required cavitation intensity without any constraints and thereby eliminating any heat generation due to sliding contact and abrasion of materials. An aluminium holder marked as number 4 in Fig. 1 was designed and manufactured to firmly hold the transducer setup and as well as to move along with the motion generated by the tribometer to apply and withdraw loads during the start and end of the test.

All experiments were performed after cleaning the test chamber by flushing with acetone to ensure no presence of any debris. The transducer was first positioned followed by placing the lower balls in the test chamber and test sample in the collet of the tribometer spindle. Lubricant was then supplied to the chamber and a sufficient level of lubricant was ensured during testing. Rotational speed, loads, test duration and cavitation intensity were set with the corresponding controls. All experiments were performed at room temperature and a forced air cooling was used to control the heating of the transducer to operate at its recommended temperature of below 50 °C. At the end of each test, the samples were removed and cleaned using an ultrasonic bath before set for surface analysis. Surface analysis was carried out with the help of optical and scanning electron microscope. The conducted test programme is described in Table 1.

3. Experimental observations

3.1. Erosion in rolling contact

Experiments carried out using this testing methodology showed cavitation erosion on the contact track in a short period of testing. Result of one of these tests is shown in Fig. 2. This was a hybrid contact test of specimen T-1, i.e. upper ball was silicon nitride and lower balls were bearing steel. Surface investigation after a couple of hours showed clearly visible erosion pits on the contact track. As shown in Fig. 2 after 3.5×10^5 stress cycles, erosion marks are only seen on the contact track and the rest of the test specimen showed no surface change. This proves that these wear marks are not generated only by cavitation, but by a combined effect of cavitation with rolling contact. The reason for formation of erosion marks only on the contact track is due to the surface changes because of contact stress coupled with rotation. During the increase in the number of stress cycles the surface gets

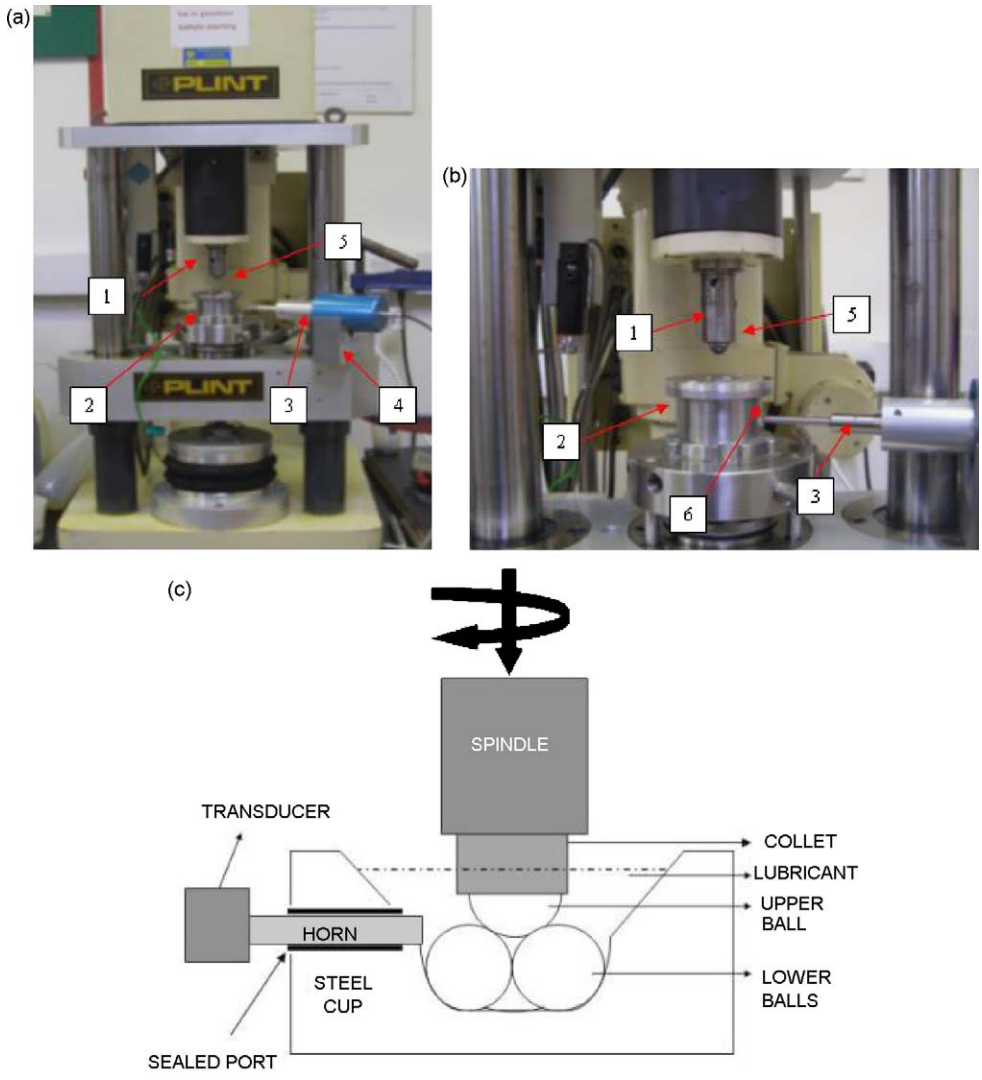

Fig. 1. (a) Experimental setup and (b) close-up of test chamber, as marked (1) machine spindle, (2) test chamber, (3) piezoelectric transducer, (4) transducer positioning holder, (5) test specimen, (6) port. (c) Schematic of the mechano-erosion experimental setup.

rougher and no longer remained smooth as the rest of the test specimen. It is well known that rough surface is vulnerable to cavitation as it accelerates the erosion process compared to a smooth polished surface [16]. Low viscosity synthetic lubricating oil (Shell Macron 110) was used for these tests, and the contact stress for this test was 3 GPa at a maximum shaft speed of 3000 rpm.

Experiments on T-3 and T-4 which were hybrid and ceramic contacts were conducted without cavitation in this test set up. These tests showed no signs of surface changes and remained

Table 1
Experiments: test programme.

Test	Contact stress (GPa)	Shaft speed (rpm)	Lubricant	Vibration amplitude (μm)	Stress cycles	Test time (min)	Material wear
T-1	3	3000	Synthetic oil	60	3.57×10^5	120	Yes
T-2	5	7000	Synthetic oil	60	1.26×10^6	180	Yes – severe
T-3	5	3000	Synthetic oil	0	1.08×10^6	360	No
T-4	3	7000	Synthetic oil	0	1.68×10^6	240	No
T-5	3	3000	Synthetic oil	60	7.63×10^5	240	Yes – less
T-6	5.1	2000	Synthetic oil	60	8.20×10^4	40	Yes – less
T-7	5.1	3000	Synthetic oil	60	5.25×10^5	180	Yes
T-8	5	5000	Synthetic oil	60	1.20×10^6	240	Yes – severe
T-9	5	3000	Synthetic oil	60	1.08×10^6	360	Yes
T-10	5	5000	Synthetic oil	60	9.30×10^5	180	Yes

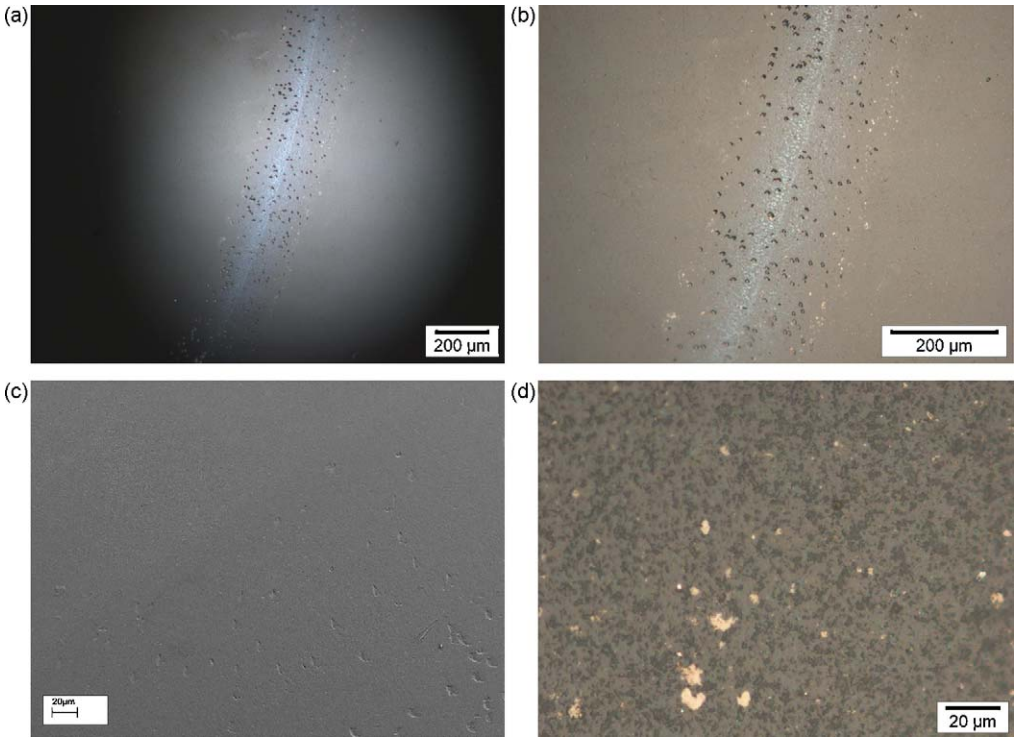

Fig. 2. (a) and (b) Erosion pits on contact track observed in T-1. (c) Edge of the contact track showing decrease in erosion pits of T-1 and (d) erosion pits T-2 (full ceramic contact).

smooth, clearly suggesting that the wear mechanism is not initiated due to rolling contact alone. With cavitation turned on, the erosion pit density was high on the contact track. A scanning electron microscope image of the edge of this contact track is shown in Fig. 2(c) and (d) of the test specimens T-1 and T-2. It is clearly seen that the population of erosion pits gradually reduce as from the centre of the contact track towards the outer region. Also the erosion pits show directionality in their geometry due to rolling induced kinetics.

3.1.1. Damage initiation observations

In static erosion cavitation tests on ceramics, the erosive wear mechanism due to cavitation consists of formation of micro-cracks and pits which then followed by pit growth developing into large pits leading to a heavy loss of material

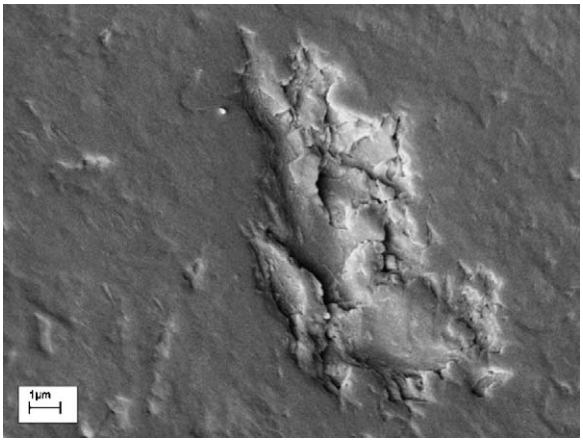

Fig. 3. Blister formation in rolling contact test T-5.

[17]. But here, the damage process and kinetics are more complicated. Few tests were carried out at different conditions to find out erosive wear initiation and progression in rolling contact. Frequent surface analysis on the test specimen was carried out to highlight the erosion initiation stage. Result of test T-5, which was hybrid contact, is shown in Fig. 3, this was tested at low load and speed for 7.63×10^5 stress cycles. The beginning stage of wear does not show any signs of micro-crack formation rather only blistering features due to mechanical impact of bubble loads. This blister of the surface layer then underwent cracking allowing the lubricant to squeeze in due to rolling contact and further rolling extricated these weakened parts. In later stages, continued testing resulted in formation of numerous pits of high concentration in the track and mild wear at the edges in the formation erosion pits.

During these initial stages, the surface became very rough which showed signs of micro-pit formation. The blister formation was found to be the main initial mechanism before micro-pit formation. This process of blistering on the surface layer is much localized in the scale of few microns due to the nature of cavitation impact loads. Once this blistering occurs, they form micro-cracks at this area showing signs of fracture. This material removal leads to the formation of micro-erosion pits. The C-shaped marks shown in Fig. 4 was caused by kinematics damage, which during continued testing allow displacing the material at this region causing the formation of C-shaped marks.

3.1.2. Erosion pits and material failure

The formation of erosion pits gradually increased as testing continued. Thus several new erosion pits were formed during

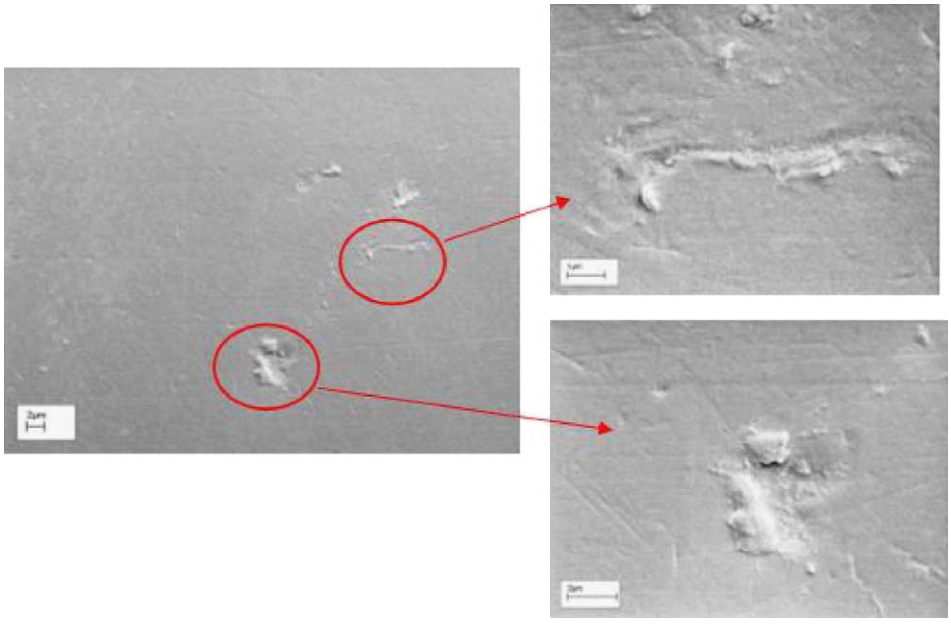

Fig. 4. Wear initiations in rolling contact as observed in test T-6.

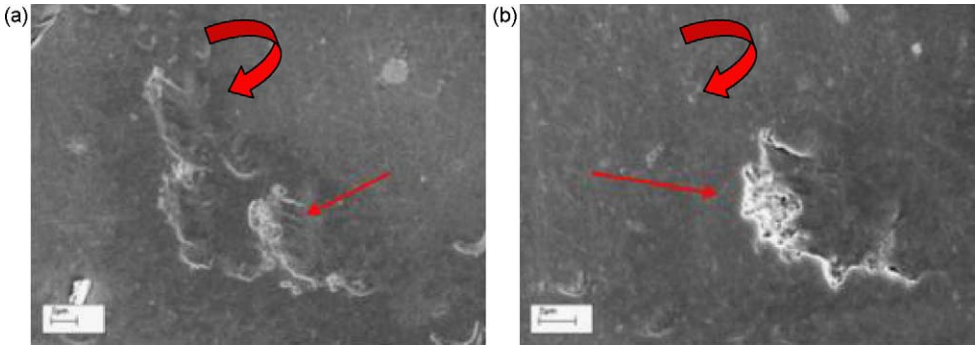

Fig. 5. Formation of C-shaped erosion marks.

the course of testing along with the earlier ones. These erosion marks are mainly characterised by C-shaped structure clearly showing the directionality due to rolling contact. The thick arrows in Fig. 5 show the direction of rotation. This is test T-7, a hybrid contact, which was tested for 5.2×10^5 stress cycles at a contact pressure of 5.1 GPa. The damage acceleration is mainly due to the process called as pit bridging as marked in Fig. 5(a). Also, the edges of these C-marks open up during rolling in the opposite direction and gets broader as marked in Fig. 5(b).

The edge of this C-mark gets wider during the course of testing which leads to the formation of micro-pits. These micro-pits then grow during further exposure to this mechano-erosion testing. This leads to erosion severity eventually causing the severe damage to the test material. Results of test specimen T-8, hybrid contact tested for 1.2×10^6 stress cycles at 5 GPa contact pressure is shown in Fig. 6. As marked in Fig. 6(a) the smooth area shows the worn out region resulting in polishing wear due to rolling contact and a large pit corresponding to the

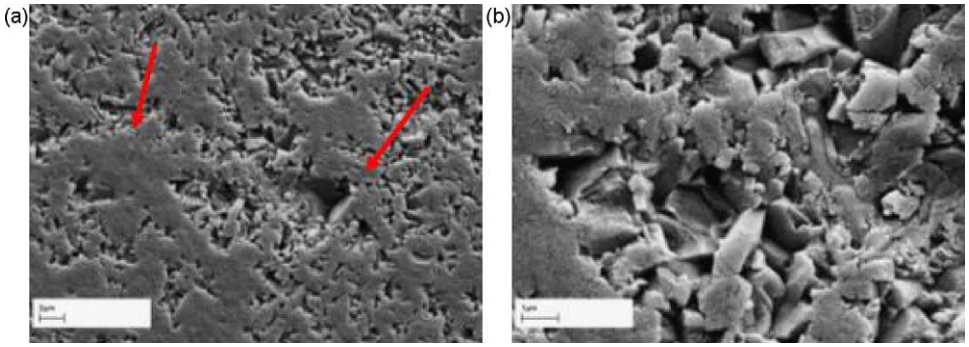

Fig. 6. (a) Final stages of erosion in rolling contact and (b) close-up.

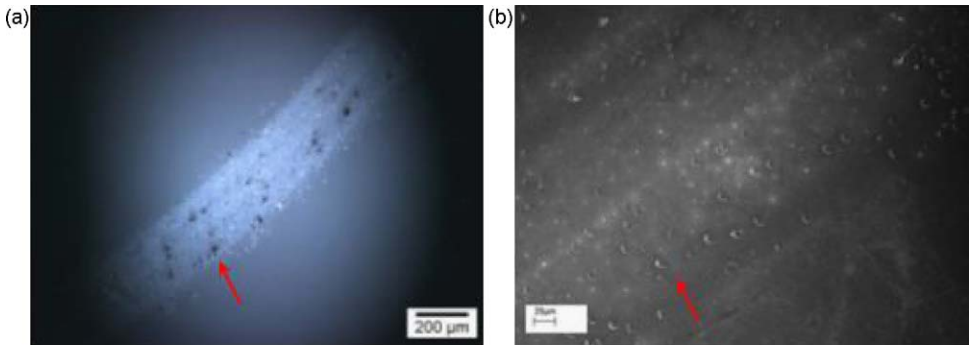

Fig. 7. (a) Ceramic contact: T-9 and (b) hybrid contact: T-10.

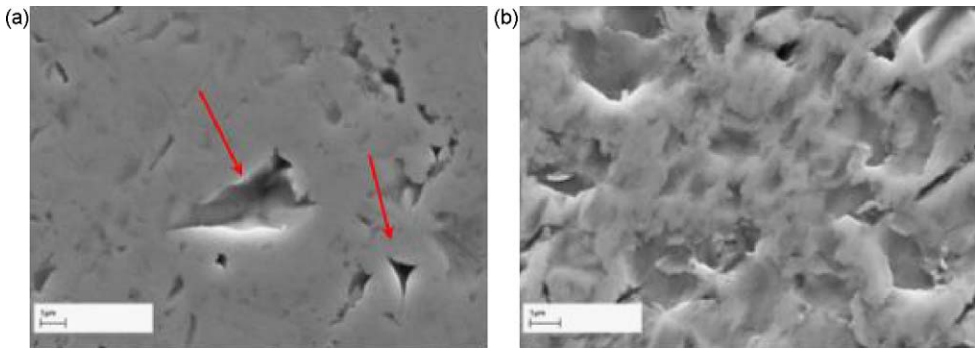

Fig. 8. Erosion in bearing steel (a) sharp erosion pits and pit bridging and (b) high density of erosion pits.

displacement of grain or bunch of grains and the adjacent areas show pit enlargement. The surface also becomes very rough. Fig. 6(b) shows the high magnification scanning electron microscope image on the final stage of the material failure.

3.2. Hybrid and ceramic contact

Different contacts, namely hybrid and ceramic to ceramic contact were investigated to understand the difference in the nature of erosion initiation and progression. As silicon nitride provides less resistance to cavitation compared to bearing steel and hence the severity of material damage was found to be high in this contact. Another major difference apart from the rate of material damage is the geometry of erosion pits. In ceramic contact, the erosion marks were observed as mere spherical in shape; whereas in hybrid contact they always exhibit the C-shaped marks as marked in Fig. 7. This formation of different shape of erosion marks clearly signifies that erosion pits do not capture the bubble cavity characteristics. Rather, this is largely influenced by the contacting material microstructure and testing conditions such as kinetics and loads in these experiments.

The contact track of the lower steel balls with ceramic upper ball was examined to understand their damage which is shown in Fig. 8. This clearly shows sharp and broad erosion pits with depth below 5 μm. This damage features are typical characteristics of erosion damage. There is also the process of pit bridging in steel as marked in Fig. 8(a). The sharper pits are similar to surface indents, which is also a characteristic of erosion in metals. Erosion on lower balls suggests that they also undergo cavitation erosion but the rate is very less compared to the test specimen which is the upper ball.

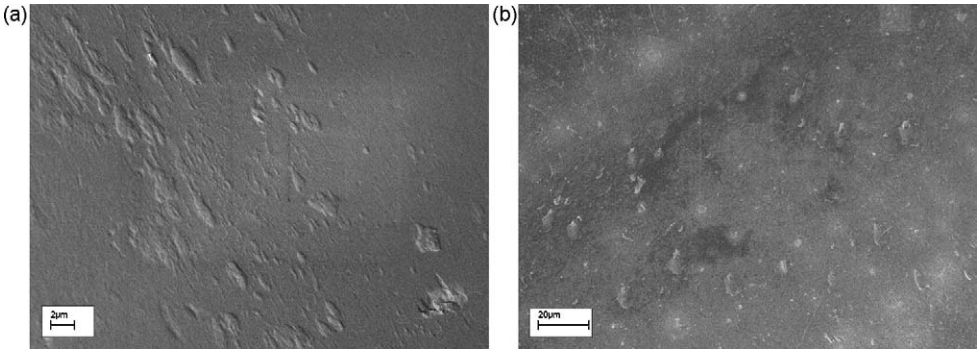

Fig. 9. Effect of contact stress (a) contact track at high load of 5.2 GPa and (b) contact track at low load of 3.5 GPa.

3.3. Effect of rolling contact test parameters

Series of experiments were performed to study the effect of test parameters on the material damage. This can be divided as (i) rolling contact fatigue and (ii) cavitation conditions. For rolling contact fatigue testing, rotational speed and the contact stress are the two key test parameters. It was found that any variation in the contact stress largely influenced the nature of cavitation erosion pit formation. At low loads of less than 3 GPa contact stress, the erosion marks were not shallower compared to the test results obtained for high loads. Fig. 9 shows results of test specimen experimented at a low load of 3 GPa and at a speed of 5000 rpm. As seen in Fig. 9(b), the number of erosion pits are high on the contact track but did not grow deeper. But the result of similar experiment shown in Fig. 9(a) with an increased contact stress of 5.2 GPa show deep and elongated erosion pit growth. Optical microscopy observations show that increase in contact pressure between the rolling elements results in deep and broad erosion marks. This is because increase in load increases the contact radius and stresses. The effect of rotational speed is very clear as the increase in speed increases the number of stress cycles thereby accelerating the damage. The increase in the number of stress cycles accelerates the surface roughness and thereby encouraging cavitation erosion.

3.4. Effect of cavitation conditions

The effect of cavitation intensity in the test liquid obviously plays a major role in this wear process. This can be easily understood by turning off the piezoelectric transducer or set it to zero amplitude of vibration. As the vibration amplitude of the transducer was gradually increased the rate of erosion increased accordingly. The cavitation intensity in the test liquid is determined by the acoustic power generated by the transducer which is directly proportional to its vibration amplitude. Below the vibration of 30 μm peak-to-peak, no erosion signs were observed on the test sample for more than 6 h and test were discontinued after this time. The sufficient level of cavitation in the test chamber is reached when the transducer vibration exceeds this 30 μm limit. Further increase in the cavitation intensity increases the material damage. This means that material damage occur only when the bubble cavity collapse is on or very close to the target surface. This concludes that the cavitation intensity is directly proportional to the rate of material wear process.

The effect of cavitation medium, which is mainly the viscosity of test liquid, has a strong influence on the rate of material damage. Different lubricants of varying viscosity as given in Table 2 were examined for this purpose. All these tests were performed at a constant speed and contact pressure of 5000 rpm and 5.2 GPa. The vibration of the transducer was set at the maximum of 60 μm. The test lubricant with a very low viscosity showed a rapid formation of erosion marks on the contact track compared to high viscous lubricant. Distilled water, which is lowest of all test lubricants showed erosion marks within 2×10^5 stress cycles. Tests on Macron 110 lubricant showed almost similar time as distilled water to form erosion pits in 1 h of exposure to mechano-erosion testing. A refrigeration oil with a Kinematic viscosity of 32 cSt showed formation of a few number of erosion marks on the contact track after 6 h of testing. Tests on other high viscous lubricants such as base oil and cylinder oil did not show any signs of erosion for a long time and hence these tests were discontinued. This clearly suggests that viscosity has a strong influence on the rate of erosion. Any increase in the viscosity of the test liquid

Table 2
Effect of lubricant viscosity.

Lubricant	Viscosity at 40 C (cSt)	Erosion initiation periods (min)
Distilled water	0.658	40
Synthetic oil	2.4	60
Gargoyle arctic	32	480
Base oil	94.6	Test discontinued
Cylinder oil	1040	Test discontinued

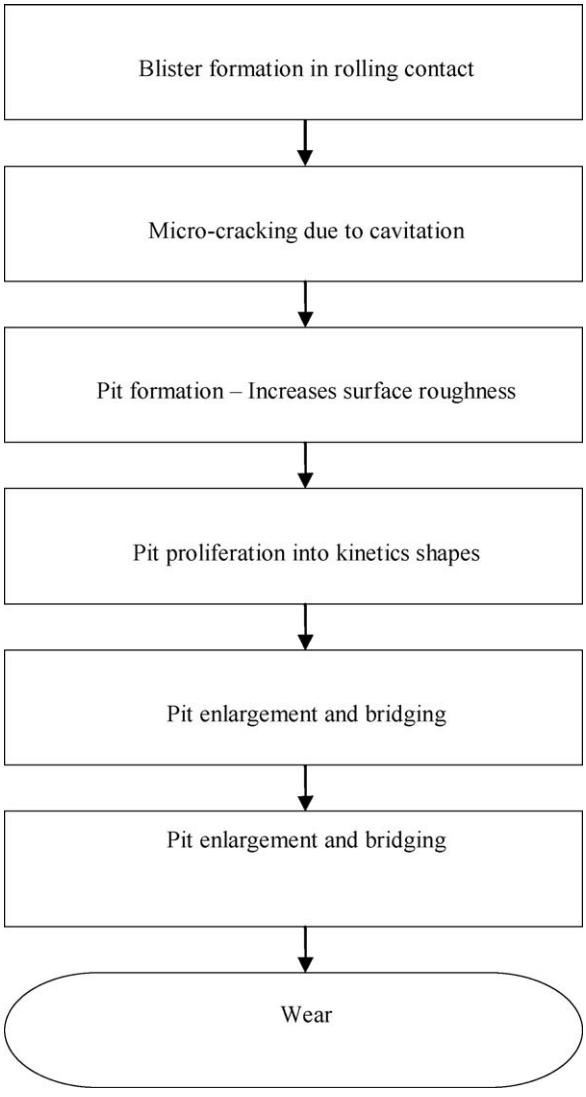

Fig. 10. Flow chart of the material wear process.

decreases the rate of erosion. The transmission of acoustic power in terms of bubble velocity from the tip of the transducer to the test material is decreased as a result of increase in lubricant viscosity. This concludes that the possibility of material wear initiation by cavitation in mechanical systems run under low viscous lubricants is very high.

4. Discussion

From these experimental results, it is clear that both cavitation and rolling contact stress played a vital role in material wear. The various steps involved in the wear initiation to severity in the rolling contact path are summarized in Fig. 10. Material wear initiated on the rolling contact path, which clearly states that cavitation and rolling contact in this region is the cause of wear development. As both these loads were applied simultaneously, the squeezing in of lubricant in the contact region allowed formation of blisters on the surface layer due to mechanical impact of bubbles. These blisters show micro-crack formation, which would allow the test liquid or lubricant to get into these micro-cracks, thereby changing the mechanism of lubrication. This change in lubrication would alter the stress distribution because of mechanical loading and also increases the hydrodynamic pressure at these regions. The passage of lubricant into these blisters accelerated erosion locally, by promoting nucleation sites for cavitation bubbles.

The C-marks formation can be attributed to the rolling direction. These marks got wider during the course of testing and hence transformed into larger pits. The final stages of material damage compromised pit enlargement and bridging, which lead to wear severity. Although the wear progress was clearly monitored on the test samples, most of the mechanisms responsible for each wear stage in this material damage are unclear. Namely, the process of lubrication changes due to the introduction of cavitation is critical, as it not only affects the rolling contact life, but would also change the wear mechanism and must be further explored. The primary mechanism of wear produced in these experiments was found to be dominated by cavitation. The secondary mechanisms such as redistribution of stresses caused by erosion pit presence and the lubricant pressure intensity at these locations are also important and must be studied.

5. Conclusion

Investigations on the combined material degradation due to erosion and rolling contact wear are presented. This mechano-erosion testing methodology proved successful in performing controlled cavitation and rolling contact experiments. Challenges in experimental study of phase changes in the lubricant and their influence on the wear mechanism are overcome by incorporating acoustic cavitation in rolling contact testing. The mechanism of material damage was identified as the characteristic of erosive wear driven by rolling contact. The effect of test parameters, such as cavitation intensity, viscosity, contact stress and rotational speed were also investigated and presented in this paper.

1. Cavitation created far away in the system is shown to be transported to the rolling contacts.
2. The plausible mechanism of material damage was by surface weakening due to mechanical impact of bubbles, which enhance fluid entrance and hydrodynamic pressure leading to blister formation. Micro-erosion pits form from these blisters and the damage accelerated by dislodging grains or bunch of grains and by pit overlapping and growth.
3. Increasing the fluid viscosity only decreased the rate of material damage, but did not alter the wear mechanism. All-ceramic and ceramic-steel contacts showed different pit morphology, suggesting that contact materials also play a vital role.
4. This testing method is suitable for a qualitative assessment of cavitation-RCF damage for different fluids with varying viscosities, and operating conditions.

Acknowledgement

The authors would like to thank Mr. Alexander de Vries, Director SKF Group Product Development, for his kind permission to publish this article.

References

[1] D. Scott, J. Blackwell, P.J. McCullagh, Silicon nitride as a rolling bearing material—a preliminary assessment, Wear 17 (1) (1971) 73–82.
[2] B. Bhushan, L.B. Sibley, Silicon nitride rolling bearings for extreme operating conditions, ASLE Trans. 25 (4) (1982) 417–428.
[3] H. Aramaki, Y. Shoda, Y. Morishita, T. Sawamoto, The performance of ball bearings with silicon-nitride ceramic balls in high speed spindles for machine tools, J. Tribol. 110 (1988) 693–698.
[4] M. Nosaka, M. Kikuchi, M. Oike, N. Kawai, Tribo-characteristics of cryogenic hybrid ceramic ball bearings for rocket turbopumps: bearing wear and transfer film, Tribol. Trans. 42 (1999) 106–115.
[5] M. Nosaka, S. Takada, M. Kikuchi, T. Sudo, M. Yoshida, Ultra-high-speed performance of ball bearings and annular seals in liquid hydrogen at up to 3 million DN (120,000 rpm), Tribol. Trans. 47 (2004) 43–53.
[6] H. Gibson, C. Moore, R. Thorn, Marshall space flight center high speed turbopump bearing test rig, in: 34th Aerospace Mechanisms Symposium, Goddard Space Flight Center, USA, 2000.
[7] J.W. Tichler, D. Scott, A note on the correlation between cavitation erosion and rolling contact fatigue resistance of ball bearing steels, Wear 16 (1970) 229–233.
[8] D. Scott, G.H. Mills, Spherical particles formed in rolling contact fatigue, Nature 241 (1973) 115–116.
[9] Z.A. Khan, M. Hadfield, S. Tobe, Y. Wang, Residual stress variations during rolling contact fatigue of refrigerant lubricated silicon nitride bearing elements, Ceram. Int. 32 (2006) 751–754.
[10] K. Mizuhara, T. Matsuzaki, The friction and wear behaviour in controlled alternative refrigerant atmosphere, Tribol. Trans. 37 (1) (1994) 120–128.
[11] U.J. Jonsson, N. Hansson, Lubrication limits of rolling element bearings in refrigeration compressors, Tribologia, vol. 18, no. 1, Finnish Society of Tribology, Finland, 1999, pp. 23–30.
[12] Z. Khan, M. Hadfield, Y. Wang, Pressurised chamber design for conducting rolling contact experiments with liquid refrigerant lubrication, Mater. Des. 26 (8) (2005) 680–689.
[13] C. Cinatar, Sustainable Development of Mechanical Systems Using Replacement Environmentally Acceptable Refrigerants, PhD thesis, Bournemouth University, UK, 2001.

[14] J. Kang, M. Hadfield, Comparison of four-ball and five-ball rolling contact fatigue tests on lubricated Si_3N_4/steel contact, Mater. Des. 24 (2003) 595–604.
[15] V. Manoj, K. Manohar, K. Shenoy, K. Gopinath, Developmental studies on rolling contact fatigue test rig, Wear 264 (7–8) (2007) 708–718.
[16] Y. Wang, M. Hadfield, Rolling Contact Fatigue of Ceramics, vol. 11, American Society of Testing Materials, 2002 (Section 6E).
[17] Y.M. Chen, Cavitation Erosion. ASM Handbook, Failure Analysis and Prevention, vol. 11, 2002, pp. 1002–1012.